Volume 16 (1997), number 1 pp. 31–41

COMPUTER GRAPHICS *forum*

Bulge Elimination in Convolution Surfaces

Jules Bloomenthal

Microsoft Corporation, Redmond, Washington 98052, USA
julesb@microsoft.com

Abstract

The relationship between surface bulge and several implicit blend techniques, particularly those based on convolution of a skeleton, is discussed. An examination of branching skeletons reveals that for two and three-dimensional skeletons, the surface will be bulge-free if skeletal elements are sufficiently large with respect to the convolution kernel.

Keywords and Phrases: blend, bulge, convolution, geometric modeling, implicit surface, skeleton.

1. Introduction

Implicit surfaces are useful for defining smooth objects. These objects may, however, evidence undesired bulges. In this paper we develop several new methods to eliminate bulges in convolution surfaces, a form of implicit blend previously developed[1]. Convolution surfaces are defined by distance to a base surface (*i.e., a skeleton*). Before discussing the bulge problem, we review surfaces defined by distance and their algebraic blend.

Distance surfaces are surfaces defined by distance to skeletal elements such as points, line segments, polygons, or any curve, surface, or volume. We illustrate distance to a planar curve in the figure below. Computing this distance is demanding[2,3], and often a piecewise linear approximation is substituted for the curve, as shown below, middle and right. When distance to a curve is defined for three-space, the resulting implicit surface is a generalized cylinder. For a skeleton consisting of n linear segments, a generalized cylinder with radius r may be implicitly defined by:

$$f(\boldsymbol{p}) = \min_{i}^{n} (d(\boldsymbol{p},\ segment_i)^2)/r^2 - 1 = 0, \qquad (1)$$

where d is Euclidean distance.

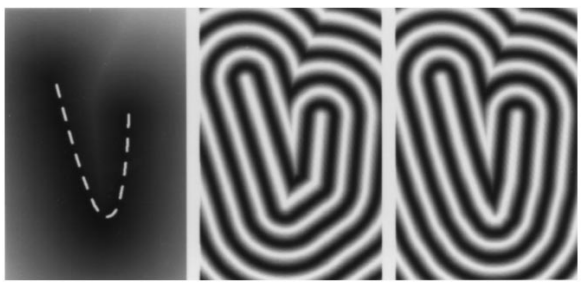

Figure 1: *Distance to Curve and to 3 and 9 Segments middle and right: contours emphasized by sinusoidal mapping*

This computation requires a single measurement for each skeletal element and a single record in memory to store the smallest distance. The result of such simplicity is that the surface encloses the simple union of the component volumes. That is, if $\boldsymbol{p}$ is within any individual $volume_i$ (defined by $segment_i$), then $d(\boldsymbol{p}, segment_i)2/r2 < 1$, $f(\boldsymbol{p}) < 0$, and $\boldsymbol{p}$ is interior to the surface. Thus, *min* in equation (1) corresponds to union, and distance surfaces may be regarded as covering the union of component volumes defined by skeletal elements.

In general, a distance surface is rounded wherever its skeleton is convex. Where the skeleton is concave (as along the upper part of the curve in Figure 1), the surface is tangent discontinuous and exhibits a crease, which we regard as undesirable. To eliminate creases, the primitive volumes must form a *blend*, rather than a union.

The blend of primitives in the context of solid modeling has received considerable study, as reported in a survey[4] and in a variety of recent work. From these

© The Eurographics Association 1997. Published by Blackwell Publishers, 108 Cowley Road, Oxford OX4 1JF, UK and 350 Main Street, Malden, MA 02148, USA.

sources we learn that blended surfaces (or *blends*) are used in mechanical design to reduce stress, improve air or water flow, simplify casting, and improve aesthetics. Implicit blends may be categorized as rolling-ball, volume-bounded, range-controlled, and global[4]. The first three produce surfaces that 'heel' to parts of individual primitive surfaces when those parts are sufficiently distant from other primitives[5].

2. Algebraic Blends

We briefly review some aspects of algebraic blends, illustrating with the range-controlled, super-elliptic blend[6]. Two primitives, P_1 and P_2, represent component volumes and are combined according to a blending function, B:

$$f(\boldsymbol{p}) = B(P_1, P_2) = 1 - \left[1 - \frac{P_1(\boldsymbol{P})}{r_1}\right]_+^t - \left[1 - \frac{P_2(\boldsymbol{P})}{r_2}\right]_+^t = 0, \quad (2)$$

where P_1, P_2 are algebraic (usually C^1 continuous) distances to skeletal elements 1 and 2, r_1 and r_2 are the 'ranges of influence' for primitives P_1 and P_2, $[x]_+$ is $max(0, x)$, and t is a user-specified parameter called the 'thumbweight.'

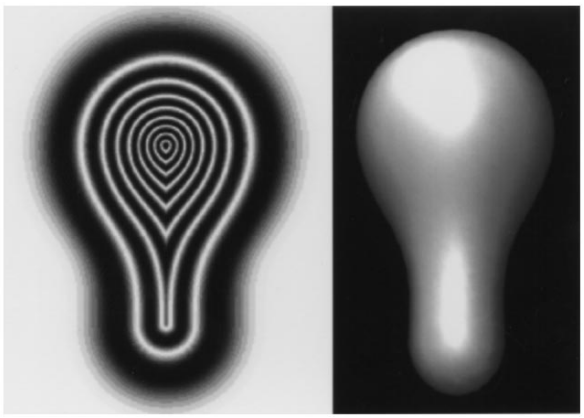

Figure 2: *Super-Elliptic Blend of Sphere and Cylinder*

The blend is called super-elliptic because the graph of $B(x, y)$ is super-elliptical (elliptical for $t = 2$). Consider an example blend[5] of the unit sphere with a cylinder (centered on the x-axis with $xB[0, 2]$ and radius .4). The sphere is given by $P_1(\boldsymbol{p}) = (\boldsymbol{p}_x^2 + \boldsymbol{p}_y^2 + \boldsymbol{p}_z^2)^{1/2} - 1$ and the cylinder is given by $P_2(\boldsymbol{p}) = (\boldsymbol{p}_x^2 + \boldsymbol{p}_y^2 + \boldsymbol{p}_z^2)^{1/2} - .4$ for $\boldsymbol{p}_x < 0$, $(\boldsymbol{p}_y^2 + \boldsymbol{p}_z^2)^{1/2} - .4$ for $0 < \boldsymbol{p}_x < 2$, and $((\boldsymbol{p}_x - 2)^2 + \boldsymbol{p}_y^2 + \boldsymbol{p}_z^2)^{1/2} - .4$ for $\boldsymbol{p}x > 2$.

The blend $f(\boldsymbol{p}) = B(P_1(\boldsymbol{p}), P_2(\boldsymbol{p}))$, for $t = 3$, is shown below, as a cross-section in the xy-plane and as a rendered surface. Although P_1 and P_2 are linear with respect to distance, B is not, which accounts for the unequal contour spacing.

No objectionable artifacts appear in the above surface, but consider now two cylinders, one along the x-axis and one along the z-axis, as shown below. Contours of the blend, in the $z = 0$ plane, exhibit a bulge where the cylinders intersect. Similar artifacts are visible elsewhere[7,8].

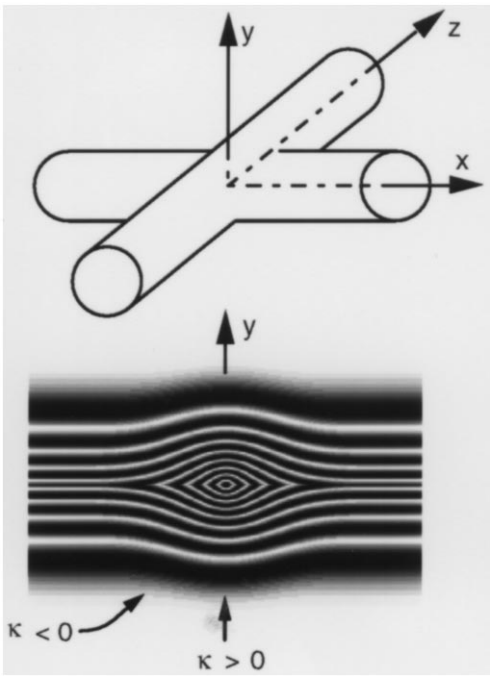

Figure 3: *Blend of Two Cylinders*

We have not encountered any formal definition of 'bulge;' therefore, we propose to define functionally 'surface bulge' as a surface surrounding a volume whose cross-section exhibits negative, then positive, then negative curvature with respect to the medial axis of the volume. This change in curvature is annotated in the figure above. For the super-elliptic blend, a bulge is to be expected, as those primitive values P_1 and P_2 that satisfy $B(P_1, P_2) = 0$ do not sum to a constant. To compensate, a modification to the blend is described5 in which the ranges of the primitive are diminished according to the angle θ between the gradients of the two primitives at a point $\boldsymbol{p}$:

$$B(P_1 P_2) = 1 - \left[1 - \frac{P_1(\boldsymbol{P})}{r_1(1 - cos\theta)}\right]_+^t - \left[1 - \frac{P_2(\boldsymbol{P})}{r_2(1 - cos\theta)}\right]_+^t. \quad (3)$$

For $\theta = 0$ the range is fully diminished and the simple

© The Eurographics Association 1997

union of the primitives results; for the concave condition $\theta = 90°$, the range is undiminished, and a blend occurs. This agrees with our observation that distance surfaces produce rounds along convex regions of a skeleton, but require blends along concave regions. $cos(\theta)$ must be non-negative, however, to avoid enlarging the primitive ranges. Possible combinations of two primitives are illustrated below.

Figure 4: *Blend of Two Segments top left: simple union, top right: bulging blend, bottom left: use of cos, bottom right: use of nonnegative cos*

The blend may be extended to k primitives[5]:

$$B_k = 1 - \sum_{i=1}^{k} \left[1 - \frac{P_i(\boldsymbol{p})}{r_i}\right]_+^t - c. \tag{4}$$

The application of Equation 3 to Equation 4 is problematic, as θ applies to two primitives only. Although primitives may be functionally composed, we consider instead convolution surfaces, a blend method based on integration, rather than algebraics.

3. Convolution Surfaces

A convolution surface is implicitly defined by a skeleton that consists of three-dimensional points, each of which contributes to $f(\boldsymbol{p})$ according to its distance from $\boldsymbol{p}$. This is reminiscent of previous work[9] in which an implicit surface is given as a summation of terms, each based on the Gaussian decay of distance to a point:

$$f(\boldsymbol{p}) = c - \sum_i e^{-\|\boldsymbol{p}-s_i\|^2/2}, \tag{5}$$

where s_i is a point on the skeleton and c is an arbitrary positive constant.

If $\{si\}$ is a set of infinitesimally spaced points, as in Figure 5, right, f can be expressed as an integral:

$$f(\boldsymbol{p}) = c - \int_s e^{-\|\boldsymbol{p}-\boldsymbol{u}\|^2/2} d\boldsymbol{u}, \tag{6}$$

where $\boldsymbol{u}$ ranges over the entire skeleton. The evaluation of the convolution integral is discussed elsewhere[1,10].

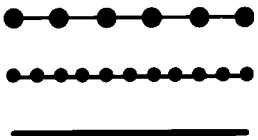

Figure 5: *Line Segment Skeleton as a Set of Points top and middle: skeleton given by increasing density of points, bottom: infinitesimally spaced points*

Convolution is a process that modifies a *signal* by a *filter*. Here, the signal is the skeleton and the filter is a three-dimensional Gaussian *kernel*. In general, the frequency components of the signal are scaled by those of the filter. This can produce various results, but low-pass filtering is the most relevant to blending. When a signal is low-pass filtered, it loses detail and is said to be *smoothed*. For example, a two-dimensional image becomes blurred and objectionable creases, such as those in Figure 1, are reduced. The effect of a filter can be shown by the *Fourier transform*, which converts a signal (such as the kernel itself) into its frequency components. The Gaussian kernel, shown below, is its own Fourier transform; thus, it attenuates the upper frequencies of the original shape to a gently increasing degree. We call a contour of the smoothed skeleton a *convolution surface*.

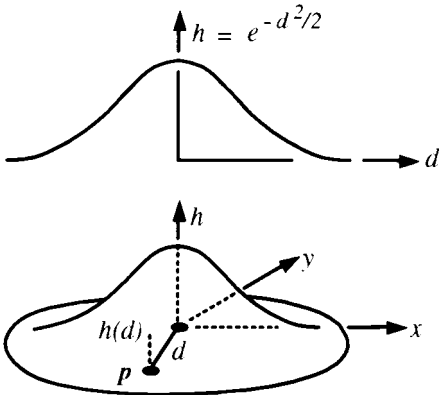

Figure 6: *The Gaussian Kernel top: one-dimensional, bottom: two-dimensional*

© The Eurographics Association 1997

Because of its property of superposition, convolution is able to smooth a shape without introducing bulges. Specifically, convolution is a linear operator, meaning the sum of individual convolutions of separate skeletal pieces is equal to the convolution of the skeleton taken as a whole; using $\otimes$ to represent convolution and h to represent the kernel, $h \otimes (s_1 + s_2) = (h \otimes s_1) + (h \otimes s_2)$. This guarantees, for example, that two abutting, colinear segments, shown below, produce the same convolution as the single segment that is their union. Accordingly, the arbitrary division of a skeleton into elements does not introduce any seam or bulge in the surface near the joins of the elements.

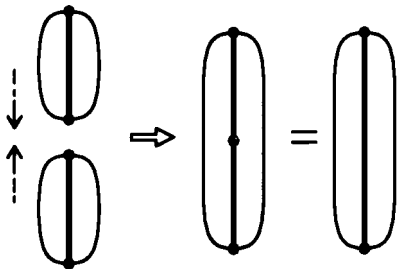

Figure 7: *The Superposition Property left: two individual line segments are brought together middle: sum of convolutions of the two segments right: convolution of a single segment*

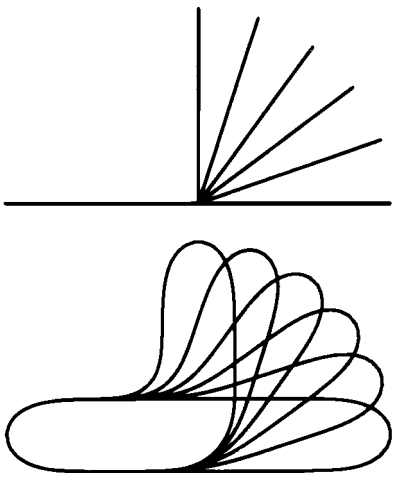

Figure 8: *Two Segments and their Convolution with the Gaussian Kernel*

The contours below illustrate convolution applied to two segments; the result is smooth regardless of the angle between the segments. Along convex portions of the skeleton, the surface mimics the union operator; along concave portions, the surface yields a blend. For isolated convex skeletons, such as a triangle or a segment, convolution produces shapes similar to distance surfaces. For complex skeletons, however, neighboring primitives blend without seam or bulge.

If the exponent in Equations 5 and 6 is scaled by π, the kernel will have unit integral; that is, the area under the curve (Figure 6, top) and the volume under the surface (Figure 6, bottom) will both be one. This implies that a signal modified by the kernel will maintain its original energy. For example, if a unit amplitude box function (whose width exceeds the full filter support) is convolved with a unit integral kernel, the peak amplitude will be one. Or, if a two-dimensional image is convolved, the overall energy in the image will be preserved. A kernel with integral less than one attenuates a signal; a kernel with integral greater than one amplifies a signal.

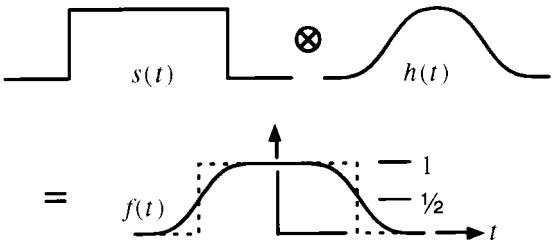

Figure 9: *Convolution of a Box Function with Unit Integral Kernel*

Because the Gaussian is symmetric, the convolution equals $\frac{1}{2}$ where the box function undergoes transition. Thus, for an iso-surface contour level of $\frac{1}{2}$, the convolution surface passes through the endpoints of skeletal segments (as shown in Figure 7) and through the edges of skeletal polygons. Accordingly, we express the convolution surface as:

$$f(\boldsymbol{p}) = \frac{1}{2} - (h \otimes s)(\boldsymbol{p}). \tag{7}$$

4. Branching Objects

Consider a branching skeleton that is organized into parent and child curves. We can give the implicit surface function as the parent curve function or the summation of the child curve functions, whichever is greater:

$$f(\boldsymbol{p}) = max\,(f_{curve}(\boldsymbol{p}, parent), \sum_{i}^{n} f_{curve}(\boldsymbol{p}, child_i). \tag{8}$$

Here $f_{segment}$ is some function of distance from $\boldsymbol{p}$ to a curve and n is the number of child curves. To maintain continuity of radii, the radius of *parent* is scaled such that in the plane perpendicular to *parent*, at its endpoint,

© The Eurographics Association 1997

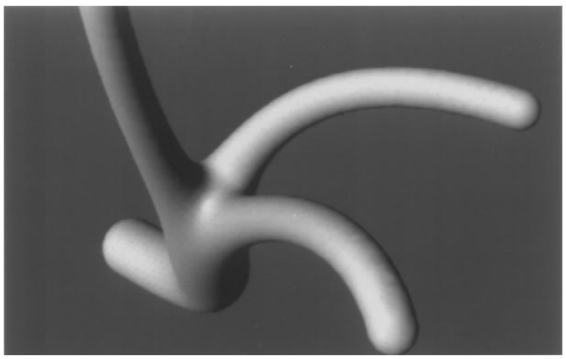

Figure 10: *A Trifurcated Ramiform*

$f_{curve}(parent) = \Sigma f_{curve}(child_i)$. As a consequence of the summation, the parent branch will be thicker than any child branch. This is another instance of implicit surface bulge; we now consider whether convolution might eliminate it.

We first examine a simple 'tee' skeleton, below, that consists of two segments. In isolation, each primitive cylinder has radius r. Application of a Gaussian filter yields slight bulges near the segment junction in both planes, below.

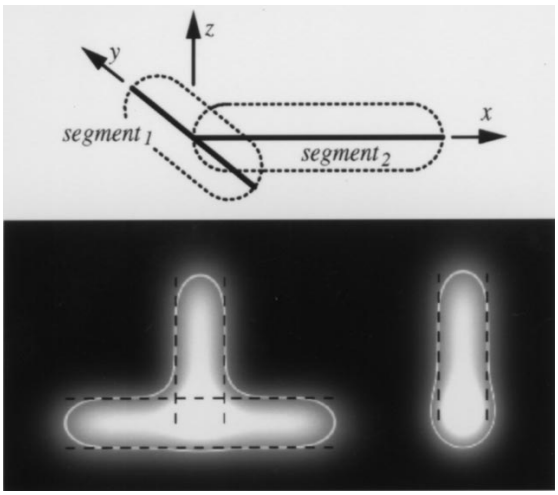

Figure 11: *A Tee top: skeletal geometry bottom: contours in xy-plane (left) and xz-plane (right) (dashed lines in contour images indicate individual primitives)*

To understand this phenomenon better, consider the behavior of $f(\boldsymbol{p})$ for points $\boldsymbol{p} = (x, 0, r)$, shown below. As x increases and $\boldsymbol{p}$ moves along the line $z = r$, the convolution of the two segments, measured at $\boldsymbol{p}$, changes. This is graphed below and predicts the bulge at the junction of the two segments. Note that the graphs for $segment_1$ and $segment_2$ are not the same along $z = r$; because $segment_1$ is perpendicular to $z = r$, the graph of its convolution reproduces the filter kernel itself, and, because $segment_2$ is parallel to $z = r$, its graph reproduces the integral of the kernel. It is this difference that produces the bulge (additional details are given elsewhere[10]).

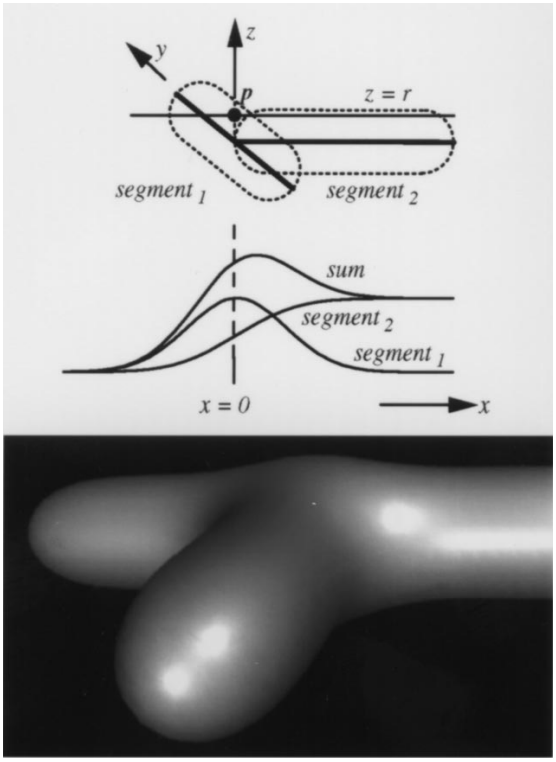

Figure 12: *Bulge at Tee Junction the bulge is indicated by the sum of the individual convolutions*

It is possible to reduce the bulge by separating the segments. If $segment_2$ is moved to the right by r, as shown below, the sum, although not constant, shows less variation than in Figure 12. The bulge and dip predicted by the graph of the sum, although subtle, are visible in the shaded close-up.

5. An Ad Hoc Approach

Figures 12 and 13 suggest a blend is needed for $\boldsymbol{p}$ within the plane of the tee, but is undesirable for $\boldsymbol{p}$ out of the plane. By interpolating between the union and blend surfaces, the following 'combination surface' can be produced.

In particular, the angle between the plane normal and the vector from $\boldsymbol{p}$ to the join of the tee controls the blend.

© The Eurographics Association 1997

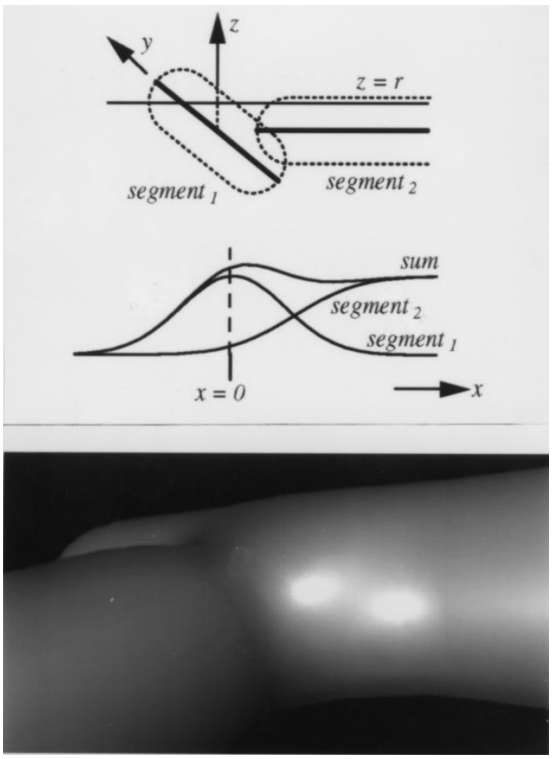

Figure 13: *Tee with Separated Segments*

If the angle is 0, then $\boldsymbol{p}$ is perpendicular to the plane and the union of the two cylinders is computed; if the angle is 90, then $\boldsymbol{p}$ is in the plane and the blend is computed. As the angle varies, the union and convolution surfaces are interpolated, reminiscent of Equation 3. The combination surface may be implemented for a skeleton by associating an approximating plane with each skeletal joint. Alternatively, a free-form surface, rather than a plane, could be fit to the vertices of a joint.

As discussed elsewhere[10], the 'webbing' that blends pairs of limbs contains a small crease. This does not appear objectionable in the above image, but motivates additional investigation.

We now consider two- and three-dimensional skeletal elements.

6. Two Dimensional Skeletal Elements

Objects with non-circular cross-sections have been accommodated by extending one-dimensional skeletal curves to two-dimensional skeletal polygons[1]. As with one-dimensional skeletons, the convolution surface for two-dimensional skeletons is evaluated as the sum of convolutions of individual skeletal elements. For example, the two polygons, below, left, yield the surface shown below, right.

Figure 14: *The Combination Surface (bottom) top: Union Surface (left) and Convolution Surface (right)*

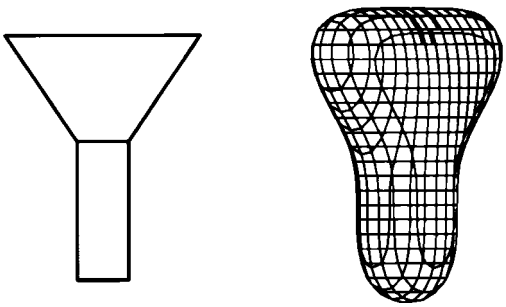

Figure 15: *Polygonal Skeleton and Convolution Surface (front and oblique views)*

A more complex application of both one and two-dimensional skeletal elements is shown below.

© The Eurographics Association 1997

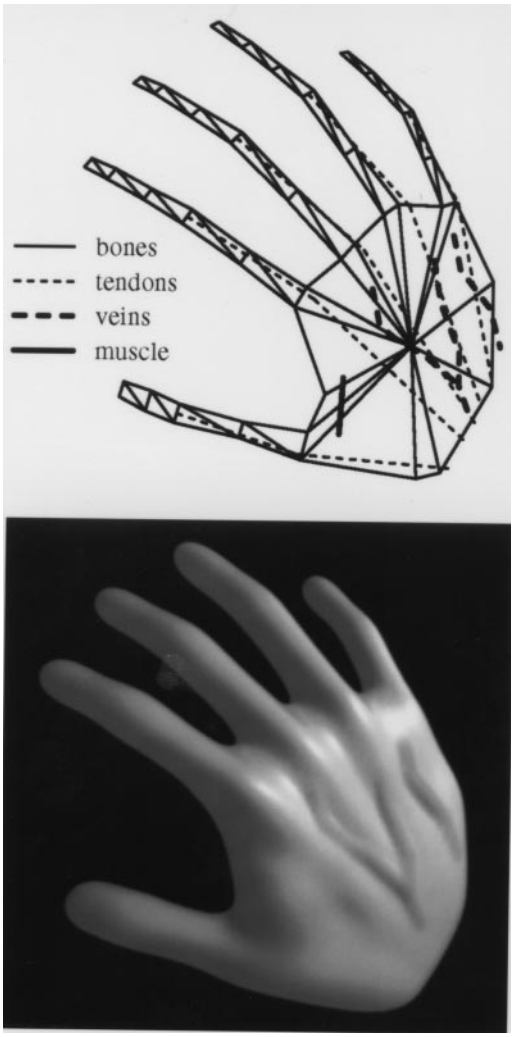

Figure 16: *Skeleton and Hand*

In Figures 15 and 16 the two dimensional skeletal elements (i.e., trapezoid, rectangle, and triangles) are contiguous with their neighbors. This is fundamental to the methods of bulge elimination we present in the remainder of this paper. One may interpret the bulges in Figures 3 and 12 as consequences of increased skeletal density; for example, in Figure 12 an endpoint of $segment_2$ touches the midpoint of $segment_1$. For polygons, a comparable arrangement is two overlapping polygons, shown below left, where the overlap indicates increased polygonal density. We speculate that a contiguous (*i.e.*, abutting and non-overlapping) skeletal arrangement, such as below right, prevents bulge. To demonstrate this, and to explain the conditions under which it is true, we examine the cross-section of a convolution surface derived from a polygon.

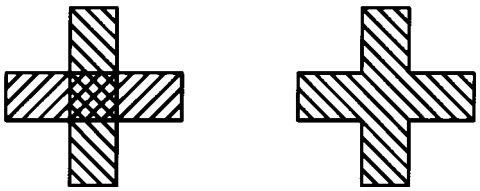

Figure 17: *Overlapped (left) and Contiguous (right) Skeletons*

As we observed in developing Equation 7, the convolution surface of a polygon can be made to pass through the polygon edges. This is a consequence of the *separability* of Equation 6; it may be written as the product of a two-dimensional integral in the plane of the polygon and a one-dimensional integral perpendicular to the plane. As described elsewhere[1], the one-dimensional integral is the kernel itself; the two-dimensional integral is the volume of the two-dimensional kernel subtended by the polygon.

Assuming the kernel is unit integral, the volume cannot reach its maximum (of 1) unless the polygon is at least as wide as $2r$ (the full support of the kernel), as shown below, top. This volume is $\frac{1}{2}$ when the kernel is directly over an edge, as shown below, bottom. In these examples we assume that the domain for the Gaussian is scaled by $\boldsymbol{\pi}$ (so that the kernel has unit integral) and that the kernel (which has infinite support) has negligible energy beyond 1.5.

To satisfy Equation 7, a point $\boldsymbol{p}$ directly over the kernel center (Figure 18, top) would be on the surface at a distance $d = h^{-1}(.5)$ from the polygon. For a monotonic kernel interpolating 0 and 1, $h^{-1}(.5)$ will necessarily be somewhere between 0 and r; for the Gaussian $h^{-1}(.5) = .46972$. Thus, for a polygon whose width is the (approximate) full-support of the Gaussian, the surface thickness will be 2(.46972); the aspect ratio for such a cross-section is 3.19339. As shown below, different kernels (all scaled to have unit integral and a maximum of 1) have different supports and aspect ratios.

For each cross-section, the polygon width equals the full filter support Thus, the cross-section just reaches its maximal height at a point above the center of the polygon. A wider polygon will not change the function value for points above the polygon center, but it will create a 'plateau' along the top and bottom of the surface, as shown below. If the polygon becomes narrower than the filter support, however, there is no point above the polygon for which the kernel, integrated over the polygon, yields unity. This does change the function value for points above the polygon center, reducing the height of the cross-section, as shown.

© The Eurographics Association 1997

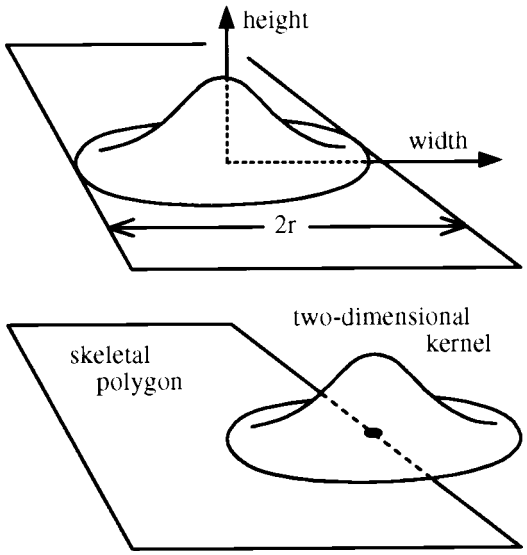

Figure 18: *A Two-Dimensional Kernel Subtended by a Polygon*

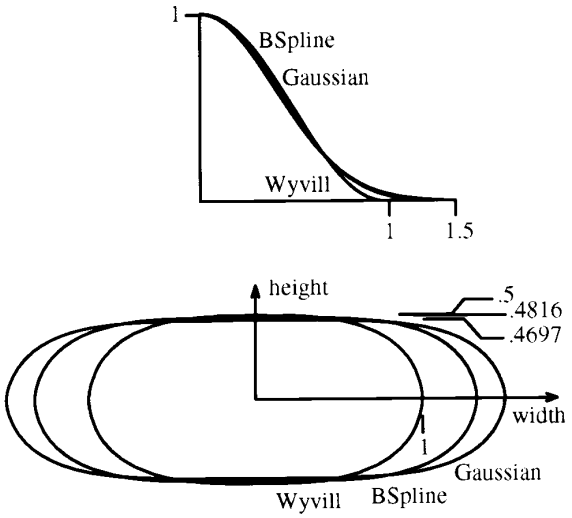

Figure 19: *Various Kernels (top) and Cross-Sections (bottom) Wyvill:* $r = 1$, $h^{-1}(\frac{1}{2}) = .5$, *aspect ratio* $= 2$ *BSpline:* $r = 1.333$, $h^{-1}(\frac{1}{2}) = .481567$ *aspect ratio* $= 2.76873$ *Gauss* $r = 1.5$, $h^{-1}(\frac{1}{2}) = .46972$, *aspect ratio* $= 3.19339$

Now, consider the contiguous skeletons shown below (each consisting of a square and four rectangles). For polygons whose width equals the support of the filter kernel, the entire filter (represented as a circle) just fits inside the polygon, and the very centers of the polygons will yield a surface of maximal thickness. For the wider

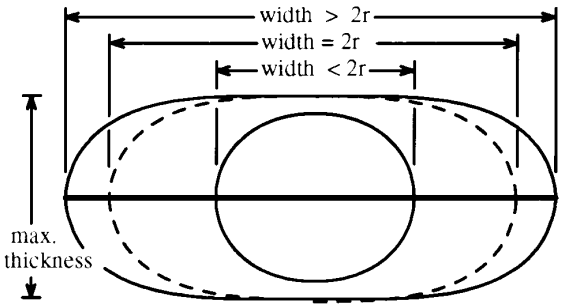

Figure 20: *Wide and Narrow Polygons*

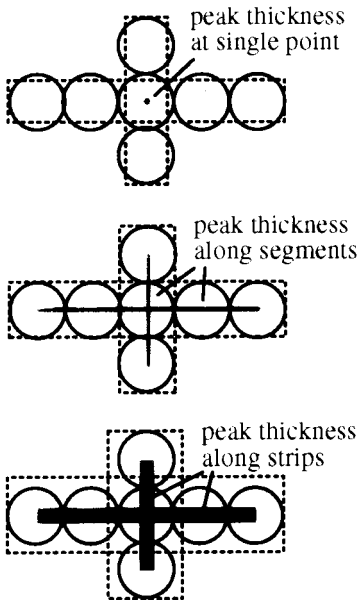

Figure 21: *Effect of Varying Polygon Width*

polygon, the region of maximal thickness widens, creating a plateau. But for the narrower polygon, only at the junction center is there sufficient room for an entire kernel; elsewhere the kernel is clipped. A bulge will occur at the center of the junction of the narrow polygons; bulges will not occur for the other polygons.

Thus, for an appropriate choice of polygon width, a contiguous, branching polygonal skeleton yields branching objects without bulge. To illustrate, the above middle skeleton is articulated, below.

Unlike cylinders derived from line segment skeletons, the cross-sections of these surfaces are oblong. This is necessarily so; in order for the two-dimensional integral term (given in the plane of the polygon) to reach its maximum, a polygon must be $2r$ wide, whereas the

© The Eurographics Association 1997

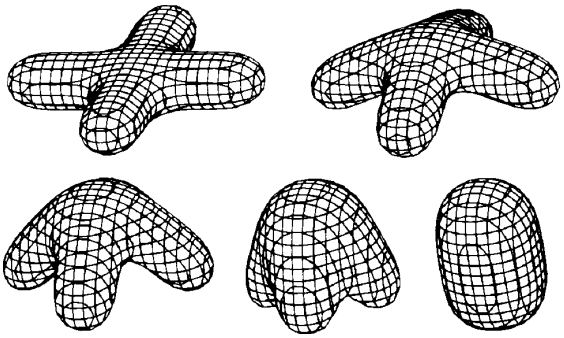

Figure 22: *A Smoothly Folding, Bulge-Free Form*

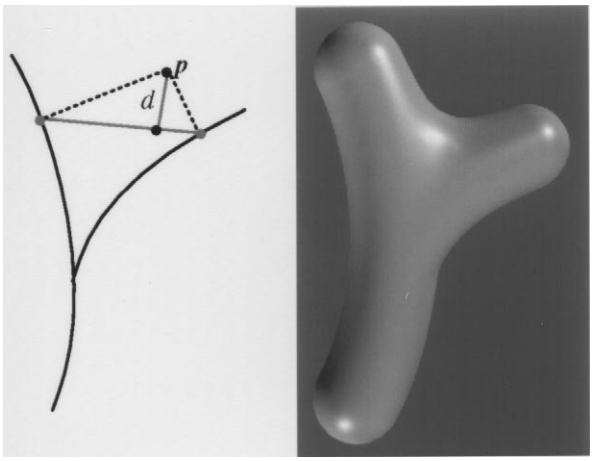

Figure 23: *A Two-Ramiform with Constant Radii left: evaluation of $f(\boldsymbol{p})$, right: shaded surface*

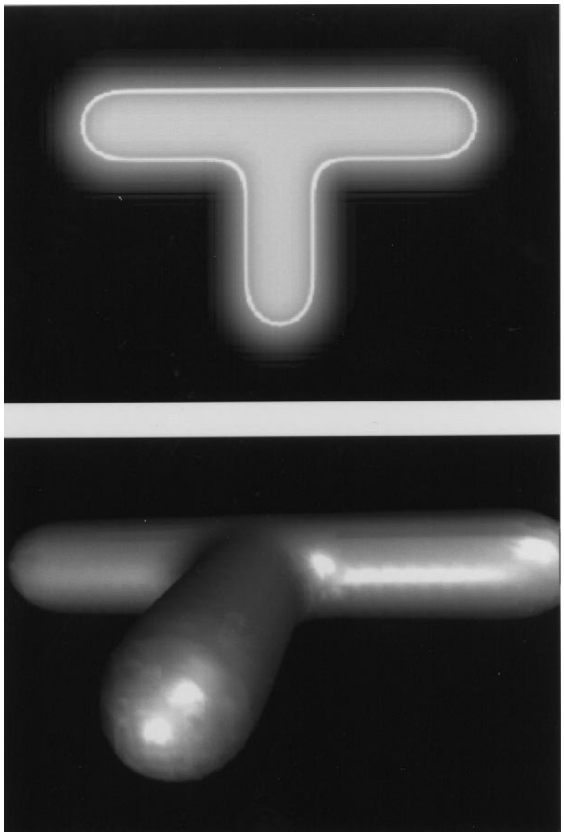

Figure 24: *Surface from Three-Dimensional Skeleton top: xy slice (iso-contour emphasized) bottom: bulge-free blend with circular cross-section*

one-dimensional integral term (given in the plane perpendicular to the polygon) can achieve any of its values within a domain or r.

7. Another Ad Hoc Approach

In previous work[11] a two-way branch is defined by d, the distance from p to the segment joining the projections of $\boldsymbol{p}$ onto the branches. This produces a bulge-free object with limbs of equal radius and circular cross-section. This method is not, however, readily extended to n-way branches.

We conclude our investigation of bulge-free objects with an examination of three-dimensional skeletons.

8. Three Dimensional Skeletal Elements

A three-dimensional skeleton can be any arbitrary volume, represented either by a dataset or by a continuous function. In particular, the skeleton can be the union surface (defined by Equation 1) and its interior; in effect, this yields the convolution of the union surface with the filter kernel. This approach has been used to smooth machine parts and thereby reduce mechanical stress; the implementation involves ray-casting to compute the convolution integral[12]. Similar smoothing has been applied in the voxel domain to reduce aliasing[13] and to produce organic appearances[14]. In this paper we note that, to avoid bulge, the primitives must have a diameter as great as the (full) filter support.

We represent the three-dimensional skeleton by a uniformly spaced voxel grid. Each grid value is weighted by the coverage of the voxel by the skeletal solid. This may be computed analytically for certain primitives, or estimated numerically by sampling within the space of each voxel. To apply the filter, each voxel propagates its weight to neighboring voxels according to its distance from the neighbor. Because voxels are points rather than line segments (which require an integral) or

© The Eurographics Association 1997

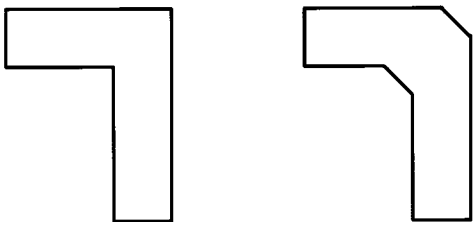

Figure 25: *Smoothing a Skeleton*

polygons (which require a two-dimensional integral), the value propagated is simply the voxel weight multiplied by the kernel value at the given distance. A 98 by 32 by 65 grid was used to compute the following images.

Although the voxel method is simple, it has relatively large memory requirements. Further, surface normals are numerically sensitive and second order interpolation of voxel values is required. Lastly, the estimation of voxel coverage by a skeletal element is compute intensive; future work might include the adaptive distribution of sample points near the boundary of the skeletal element.

9. Conclusion

This paper has examined various implicit blends, focusing on convolution surfaces. Because convolution is an integration, it produces a blend of primitive volumes; the resulting object appears pliable. The object is not without structure, however; blending occurs only where skeletal elements are in proximity, and other parts of the surface closely follow the skeletal structure. Seams do not occur where skeletal elements meet. As with algebraic blends, convolution surfaces are prone to bulge when applied to branching skeletons. Provided the skeletal elements collectively span the full filter support, however, branching objects are bulge-free.

The restriction that skeletal diameter must equal or exceed the filter support may contradict design requirements. In these cases, it may be possible to alter the skeleton to adjust fillets and chamfers, as suggested in the illustration below.

We speculate that one-dimensional segments or curves, two-dimensional polygons or images, and three-dimensional volumes provide great flexibility for the design of convolution surfaces; the use of point skeletons is appropriate for certain forms as well[9,15,16]. There are advantages and disadvantages to each skeletal dimension. The convolution of a single point may be performed analytically, but a large number of points are required to model flat surfaces. The convolution of a line segment requires a one-dimensional integral, but bulges will arise for branching skeletons. The convolution of a polygonal skeleton can eliminate bulges, but requires a raster representation and produces oblong cross-sections. The convolution of a volume requires a voxel representation, can eliminate bulges, and can produce circular cross-sections.

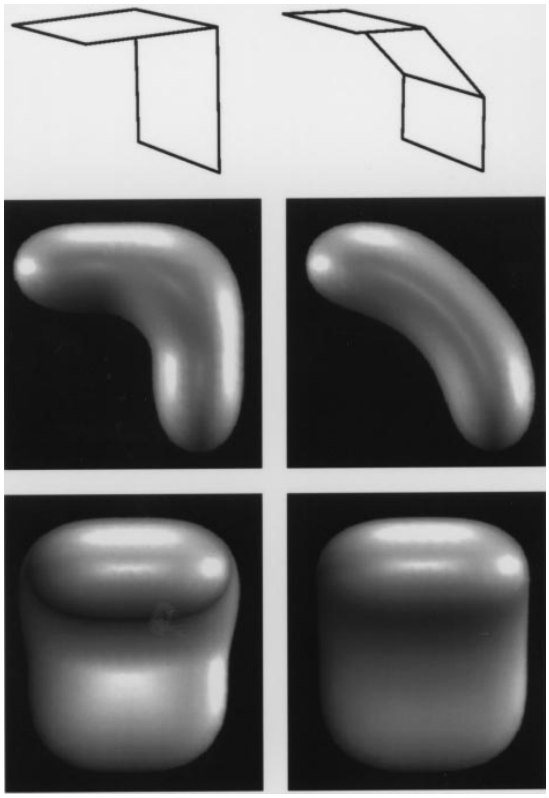

Figure 26: *Local Densities left: two element skeleton, right: three element skeleton top row: oblique views of skeletons middle and bottom rows: side and front views of surfaces*

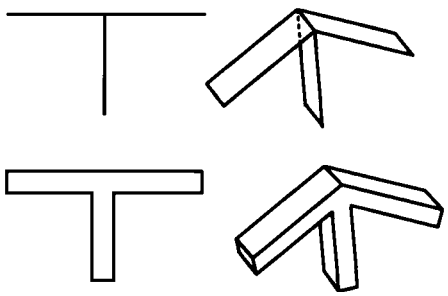

Figure 27: *One, Two, and Three-Dimensional Skeletons top: those prone to produce bulges, bottom: those less prone*

© The Eurographics Association 1997

We briefly mentioned the relation between skeletal density and bulges. Presently, this is not well understood. Although a polygonal skeleton can alleviate the bulge caused by a branching one-dimensional skeleton (Figure 12), it can produce a bulge, even without branching. As shown below, when the local density of the skeleton is more uniform, the bulge is greatly diminished.

We speculate that a skeleton distributes its density more uniformly if it is locally manifold. As illustrated below, a one-dimensional skeleton should contain no point at which three or more segments meet, and a two-dimensional skeleton should contain no edge at which three or more polygons meet.

A system utilizing convolution surfaces facilitates the design of complex, smooth, well-behaved shapes through the specification of skeletal elements. The designer may lose explicit control over fillets and chamfers, but enjoys a very forgiving and intuitively applied blend technique.

Acknowledgments

My thanks to Paul Heckbert, Przemek Prusinkiewicz, Ken Shoemake, and Brian Wyvill for their insight throughout the development and analysis of the techniques reported here. My thanks also to the reviewers for their helpful comments. And finally, my thanks to Allan Thorpe for his support during the revision of this paper.

References

1. J. Bloomenthal and K. Shoemake, *Convolution Surfaces*, Proceedings of SIGGRAPH'91, Las Vegas, NV, in Computer Graphics **25**, 4, July 1991.
2. J. Bloomenthal, *Techniques for Implicit Modeling*, Xerox PARC Technical Report P89-00106, 1989.
3. P. Schneider, *Solving the Nearest-Point-On-Curve Problem*, in Graphics Gems, Andrew Glassner, editor, Academic Press, New York, 1990.
4. J. R. Woodwark, *Blends in Geometric Modeling*, Proceedings of the 2nd IMA Conference on the Mathematics of Surfaces, Cardiff, September 1986.
5. A. Rockwood, *The Displacement Method for Implicit Blending Surfaces in Solid Models*. ACM Transactions on Graphics **8**, 4, October 1989.
6. A. Rockwood and J. C. Owen, *Blending Surfaces in Solid Modeling*, Proceedings of SIAM Conference on Geometric Modeling and Robotics, G. Farin, editor, Albany, NY, 1985.
7. C. Hoffmann and J. Hopcroft, *The Potential Method for Blending Surfaces and Corners*, Technical Report TR 85-674 Computer Science Dept., Cornell University, 1985.
8. A. E. Middleditch and K. H. Sears, *Blend Surfaces for Set Theoretic Volume Modeling Systems*, Proceedings of SIGGRAPH'85, San Francisco, CA, in Computer Graphics *19*, 3, July 1985.
9. J. Blinn, *A Generalization of Algebraic Surface Drawing*, ACM Transactions on Graphics, July 1982.
10. J. Bloomenthal, *Skeletal Design of Natural Forms*, PhD dissertation, Department of Computer Science, University of Calgary, 1995.
11. J. Bloomenthal and B. Wyvill, *Interactive Techniques for Implicit Modeling*, Symposium on Interactive 3D Computer Graphics, Snowbird, UT, in Computer Graphics, **24**, 2, March 1990.
12. S. Colburn, *Solid Modeling with Global Blending for Machining Dies and Patterns*, SAE Technical Paper Series #900878, Society of Automotive Engineers, Inc., 1990.
13. S. W. Wang and A. E. Kaufman, *Volume-Sampled 3D Modeling*, Computer Graphics and Applications, **14**, 5, September 1994.
14. J. Wilhelms, *Animals with Anatomy*, IEEE Computer Graphics and Applications, to appear, 1996.
15. S. Muraki, *Volumetric Shape Description of Range Data Using "Blobby Model",* Proceedings of SIGGRAPH'91, Las Vegas, NV, in Computer Graphics **25**, 4, July 1991.
16. G. Wyvill, C. McPheeters and B. Wyvill, *Animating Soft Objects*, The Visual Computer, **2**, 4, August 1986.

© The Eurographics Association 1997